**Atmospheric
Chemistry
and Physics
Discussions**

**Boundary layer
physics over snow
and ice**

P. S. Anderson and
W. D. Neff

Boundary layer physics over snow and ice

P. S. Anderson[1] and W. D. Neff[2]

[1]British Antarctic Survey, Cambridge, UK
[2]NOAA Earth System Research Laboratory, Boulder, Colorado, USA

Correspondence to: P. S. Anderson (philip.s.anderson@bas.ac.uk)

Title Page	
Abstract	Introduction
Conclusions	References
Tables	Figures
|◄	►|
◄	►
Back	Close

Full Screen / Esc

Printer-friendly Version

Interactive Discussion

EGU

P. S. Anderson and W. D. Neff

Abstract

A general understanding of the physics of advection and turbulent mixing within the near surface atmosphere assists the interpretation and predictive power of air chemistry theory. The theory of the physical processes involved in diffusion of trace gas re-
⁵ actants in the near surface atmosphere is still incomplete. Such boundary layer theory is least understood over snow and ice covered surfaces, due in part to the thermo-optical properties of the surface. Polar boundary layers have additional aspects to consider, due to the possibility of long periods without diurnal forcing and enhanced Coriolis effects.

¹⁰ This paper provides a review of present concepts in polar boundary layer meteorology, which will generally apply to atmospheric flow over snow and ice surfaces. It forms a companion paper to the chemistry review papers in this special issue of ACP.

1 Introduction

A variety of processes near the surface of the Earth mediate the transfer of heat, mo-
¹⁵ mentum, moisture, and chemical species between the surface and the overlying atmosphere. As a number of studies over the last decade in the polar regions have shown, these processes include a complex mixture of both vertical turbulent exchange and horizontal transport. These studies have taken place in both the coastal margins of the Arctic and the Antarctic where sea ice, open water, snow-covered coastal mar-
²⁰ gins and abrupt topographic features create a highly heterogeneous environment and over the nearly homogeneous ice surfaces characterizing the interior of Antarctica and Greenland.

This paper grew out of a request from the Air-Ice Chemical Interactions (AICI) community for a paper on the physics of the boundary layer to supplement the state-of-the-
²⁵ science papers in this special issue addressing snow photochemistry, halogens and ozone-depleting episodes, and mercury transport and deposition in the polar regions.

Such a discussion is warranted due to the interplay of physical mechanisms that may affect trace gas measurements made near the surface, especially when the surface is, itself, a source of trace gas or catalytic to reaction. An additional motivation are recent surprises such as 1) the unexpectedly high levels of nitric oxide found over the high
⁵ interior of Antarctic that appear to have origins in the formation of very shallow mixing layers coupled with photo-denitrification of the snow and 2) the complex chemistry and meteorology of the more deeply mixed ozone-deleting-episodes (ODEs) found first in the Arctic and more recently in the Antarctic. This paper is intended to serve as an introduction to the most relevant boundary layer physics and meteorology applicable to
¹⁰ such chemical phenomena, including suitable techniques for observing and quantifying the related atmospheric processes.

A number of field programs have contributed to our understanding of boundary layer processes and their relevance to ice-air chemical interactions. Several of note are:

– Neumayer: Variations in NOx gradients derived from PEAN'99 data (Photochem-
¹⁵ ical Experiment at Neumayer) were correlated with estimates of actinic flux once boundary layer activity (mixing) was considered (Jones et al., 2001). Although limited micro-meteorological data were available, turbulent diffusivity and actinic flux were inferred from standard meteorological data, indicating the role of turbulence in air chemistry near the ground. A similar study for Peroxyacetyl nitrate (PAN)
²⁰ during PEAN'99 highlighted the benefits of having co-located in situ turbulence sensors during boundary layer chemistry campaigns (Jacobi et al., 2000).

– Halley: The main air chemistry facility at Halley, the Clean Air Sector Laboratory (CASLab) deployed in the 2002/3 austral summer, is co-located with a range of turbulence and profile instrumentation within the Instrumented Clean Air Sector
²⁵ (ICAS). Micro-meteorology support data are available from a 30 m vertical array of sonic anemometers, propeller vane and aspirated temperature sensors, sodar and microbarograph array. Results from these facilities are reported elsewhere, (see ACP Special Issue, 2007), but especial note should be taken of (Jones et al.,

Boundary layer physics over snow and ice

P. S. Anderson and W. D. Neff

2006) describing the dependence of near surface ozone upon mixing or frontal events.

– South Pole: During the Investigation of Sulfur Chemistry in the Antarctic Troposphere (ISCAT) project at the South Pole in 1998, unexpectedly high near-surface concentrations of nitric oxide, [NO], were found and linked to photo-denitrification of the snow and subsequent flux of NO into the boundary layer (Davis et al., 2001). A subsequent study in the spring of 2000 suggested that the extremely high [NO] could be explained by a combination of factors including non-linear chemical processes, shallow boundary layers, and NO_x accumulation in air parcels as they drain off the high plateau toward the South Pole (Davis et al., 2004b). However, these earlier studies lacked documentation of the vertical structure of the boundary layer and associated chemical constituents. These were addressed in a third study in 2003, namely, the Antarctic Tropospheric Chemistry Investigation (ANTCI). Results now include a detailed analysis of boundary layer behaviour and depth using a sodar, tower meteorology, tethered balloon for meteorological profiling, and a sonic anemometer (Neff et al., 2007), tethered balloon profiling of NO and O_3 (Helmig et al., 2007a; Helmig et al., 2007b; Neff, 1978) numerical modeling that included simulation of boundary layer depth and chemical interactions (Wang et al., 2007). Comparison of observations of mixing layer depth, [NO], and numerical simulations suggested the need for better documentation of snow nitrate levels and the processes controlling the flux of NO from the snow. In addition, analysis of aerosol ions and trace elements suggest significant marine influences during some of the high [NO] episodes at the South Pole (Arimoto et al., 2007[1]) which raises the issue that in remote areas, we have no documentation of the boundary layer processes that occur along these extensive over-the-ice transport trajectories (Neff et al., 2007).

---

[1]Arimoto, R., Zeng, T., Khaing, H., Wang, Y., and Huey, G.: Concentrations and Sources of Aerosol Ions and Trace Elements during ANTCI-2003, Atmos. Environ., submitted, 2007.

- Arctic: Following the early discovery of ozone depleting episodes (ODEs) in the arctic (Oltmans, 1981) a number of field programs have exposed the many roles of the complex chemistry and boundary layer meteorology in the arctic as reviewed in this special issue (Simpson et al., this issue). Unlike the interior of Antarctica where shallow boundary layers dominate ice-atmosphere chemical interactions, deep mixing from both wide leads (up to 4 km, Schnell et al., 1989) as well as more modest leads with mixing to 1 km, the nominal depth of the arctic temperature inversion have been found (Kahl, 1990; Serreze et al., 1992). The depth of the ODEs has been found to be highly variable as revealed in sequential ozonesonde soundings (Shepson et al., 2003) and reflect transport, potentially from the marginal ice zone, over periods of one to three days (Bottenheim and Chan, 2006).

Section 2 provides specific and practical definitions of the Atmospheric Boundary Layer, and introduces the concept of mixing height. Section 3 summarizes the mechanisms where variation in boundary layer characteristics will affect air chemistry studies, either by modifying the chemistry itself, of by generating extrinsic signals in sample measurements. Section 4 describes the main general types of boundary layer encountered in polar field work, based on stratification and topography. Section 5 lists typical micro-meteorological field equipment, and how such additional measurements would enhance an air chemistry campaign. Section 6 summarizes the issues presented. Appendix A is a list of useful equations.

2 Defining the boundary layer

This section describes both formal and practical definitions of the boundary layer. (Stull, 1988) defines the atmospheric boundary layer as "that part of the atmosphere that is directly influenced by the presence of the earth's surface, and responds to surface forcing with a time scale of an hour or less." Such forcing includes processes affecting

the transfer of heat, momentum and moisture, the effect of terrain variations, as well as emissions of trace gases that affect the radiative balance at the surface and within the air. In the polar regions, the response to surface forcing may be much slower than an hour under very stable conditions and the Earth's rotation may play a larger role
5 because the inertial period approaches twelve hours at the poles. For air chemistry modeling studies the most significant physical boundary layer variables are height, h_z, and the profile of the diffusivity, $K(z)$. h_z indicates the volume of the reactive mixing region, whilst $K(z)$ quantifies the vertical flux of tracer given a known concentration profile, $C(z)$. Box models of boundary layer air chemistry require h_z, whilst 1-D profile
10 models (multiple or stacked box models) require $K(z)$, h_z being implicit in the $K(z)$ profile. This paper gives added weight to discussion of these two parameters.

2.1 History and formal definitions

One of the earliest concepts of a fluid boundary layer was initially proposed by Prandtl (1905) to explain the behaviour of laminar fluid flow tangential to a surface. He noted
15 that if fluid flows past a solid object without slipping, there should be both very large tangential velocity gradients, du/dz, and also large negative velocity curvature, $-d^2u/dz^2$. Diffusive theory could then be applied to this curvature, the resulting implications being that, in steady state, a horizontal decreasing pressure gradient, $-dP/dx$, must exist to balance this curvature. If the pressure gradient is reduced at any point, for instance
20 by expanding the flow rapidly in a venturi, the boundary layer will separate from the surface. This is the reason why flows are changed gradually over wings or fan blades to prevent such a separation.

Of more relevance to the topic of air chemistry was a secondary conclusion. The depth of the (molecular) boundary layer increases with distance from the "start".
25 Prandtl worked mainly with pipes or flat plates in tanks. The start of the boundary layer was known, and the length of the layer was finite. However, Prandtl's analysis indicated that the boundary layer depth would grow indefinitely. There is no inherent (molecular) boundary layer depth which depends on the local flow characteristics, it

Boundary layer physics over snow and ice

P. S. Anderson and W. D. Neff

Title Page

Abstract	Introduction
Conclusions	References
Tables	Figures

|◄| ►|
|◄| ►|

| Back | Close |

Full Screen / Esc

Printer-friendly Version

Interactive Discussion

depends where it is.

Prandtl's analysis only applies to fluids when the Reynolds Number, *Re* is small. *Re* is defined in terms of the kinematic viscosity, *v*, velocity, *V,* and a length scale of the object, *L*, e.g. the diameter of a pipe through which the fluid flows. *Re* is the dimensionless ratio of these three factors:

$$Re = \frac{LV}{\upsilon} \qquad (1)$$

For *Re*<600 the flow will be laminar. However, typical *Re* for atmospheric flows are $O(10^5)$ or more and the concept of diffusivity has to be extended to include turbulent exchange of fluid parcels rather than molecular transfer as we will describe in more detail later. However, many aspects of viscous boundary layers carry over in the conceptualization of turbulent boundary layers.

2.2   Practical and informal definitions

The literature addressing the depth of boundary layers under conditions of small *Re* is extensive and the problem is often amenable to analytical solution. However, the definition of the boundary layer depth under realistic atmospheric conditions is problematic because the magnitude and nature of the "turbulent diffusivity" responds to intrinsic properties of the flow such as wind shear and vertical temperature differences. In addition, within a stably stratified atmosphere (one where the effect of buoyancy is to try to restore a displaced air parcel back to its original position) wave motions can propagate momentum indirectly and direct turbulent transfer can be extremely weak. Furthermore, the history of the flow upstream of an observation site can determine the properties of the boundary layer at the site rather than the surface forcing at the site itself. Such non-local effects confound parameterization methods based on the local meteorological conditions.

For example, flow over leads or polynyas, openings in the ice overlying the ocean, can be modified dramatically by the local heat input (Serreze et al., 1992). On long

time scales, the rotation of the Earth will modify the behaviour of turbulent boundary layers, an effect first describe in detail by Ekman (1905).

One of the most conceptually simple definitions of the boundary layer depth is the height at which turbulence decreases to a very small value, typically 10% of its value at the surface. However, even if a definition based on mixing is valid, measuring mixing in situ above the height of a typical mast (30 m) is rarely viable. In place of direct measurements, other proxies are often used, the most popular being inspection of the temperature profile (gained from free flying or tethered balloon sondes). However, the temperature profile can be influenced by larger scale weather processes. Thus, the boundary layer may extend through only a small fraction of the depth deduced from the temperature profile, especially under stable conditions. In particular, the temperature profile technique relies on a number of effects that indicate where mixing is near zero. For instance, where initially a linear thermal gradient exists, rapid mixing will generate a volume of equalised temperature, with a sudden step at the edges, as shown in Fig. 1. Conversely, surface cooling of an initially isothermal boundary layer will generate a temperature gradient. The ease of measuring temperature gradients has biased the literature to defining the boundary layer according to the profile, and detracts from the fact that the temperature is only a proxy for mixing under limited circumstances such as in the case of convection with a capping temperature inversion.

This is of notable concern within the polar studies of the physics and chemistry of boundary layers because the bulk of boundary layer literature is based on mid-latitude data, where diurnal variations in insolation dominate the evolution of the boundary layer. Such variation may be absent or minimal in polar regions, whilst other forcing, e.g. drainage (katabatic) forcing or polynyal convection may dominate. The overuse of the term "inversion depth", "top of inversion" and "capping inversion" as identifying the top of the mixing layer may lead to incorrect conclusions regarding the depth, as well as confusing the issue as to the mechanism constraining the mixing height.

Boundary layer physics over snow and ice

P. S. Anderson and W. D. Neff

Title Page

Abstract | Introduction

Conclusions | References

Tables | Figures

◄ | ►

◄ | ►

Back | Close

Full Screen / Esc

Printer-friendly Version

Interactive Discussion

EGU

2.3 Mixing depth or boundary layer height

For chemistry boundary layer studies, knowing the mixing depth is often central to understanding the resulting concentrations of tracer, especially for gases released at the surface. For physical studies, h_z is a useful scaling function for estimating fluxes of momentum and heat. The lack of universal parameterisation schemes for estimating h_z from local meteorological variables is therefore unfortunate, and there is still active research in this subject. Ideal, simplistic models such as Prandtl, indicate that the boundary layer grows indefinitely with fetch, clearly an unrealistic assumption over virtually infinite plains. Ekman's model limits vertical extent by incorporating the Coriolis parameter whilst convection and stable stratification incorporate buoyancy (positive and negative respectively) to scale h_z. In general, however, there is poor correlation between models and measurements.

Figure 1 demonstrates the difficulty in attempts to make estimates of h_z from local measurements. Classic mid-latitude stable boundary layer temperature profiles are shown; upper left is the "nocturnal" boundary layer, which occurs on cloud free nights in mid-latitude and is caused by radiative surface cooling, whilst the upper right is the "early morning" boundary layer, where weak convection is heating the surface, but has yet to penetrate fully into the cooled overlying layer. Both of these profiles are observed in polar regions, but occasionally formed by different mechanisms. The nocturnal boundary layer profile is formed by warm air overlying a cold surface, but in polar regions this can frequently occur due to the advection of warm air, not the cooling of the surface. The mid-morning profile is very common in polar regions, for instance within or near sea-ice due to polynyal fossil convection, as described in Culf (1989) and Anderson (2003). For instance, compare Fig. 1 to the temperature profiles from Eureka, Resolute and Churchill in Tarasick and Bottenheim (2002).

Even if we were able to measure the diffusivity at all heights, some boundary layers evolve complex vertical structure. For reasons still not understood, extreme surface cooling can result in horizontal layers of turbulent and laminar air. The layers generally

evolve from a classic well defined boundary layer, with an area within the turbulent zone becoming laminar. Occasionally, the layering is generated by the apparent peeling away of the top of the mixed boundary layer into the relatively laminar air aloft. Under such circumstances, there is no valid definition of "boundary layer depth".

5   Despite the uncertainty in models and measurements of h_z, there is some consolation for air chemistry studies, in that for modeling work beyond the box model, it is the diffusivity near the surface that is of most interest, and this can be more easily determined, whether by direct measurement, or via proxies.

3   How the ABL affects air chemistry observations

10 Micro-meteorological mechanisms affecting trace gas observations may divided into two broad categories: vertical mixing and horizontal transport. Mixing is the most apparent characteristic, whilst transport, or advection, can be all too easily disregarded when observations are made at only one point.

3.1   Horizontal transport: advection

15 Under all but calm wind conditions, by definition the boundary layer winds have a net horizontal component, which can have both an actual and an apparent effect on trace gas observations. An example of an apparent effect is when the boundary between two air masses passes over the sampling site. Figure 2 shows an idealised 2-D flow field, viewed from above, of two rotating air masses; the sampling point is slightly off centre.

20 Small relative changes in the positions of the sample site to the air masses movements may cause the sampler to cross the boundary between the air masses, with no significant change in wind speed or direction. If the two air masses have different chemical signatures, the sampling point would observe a rapid change in air composition. It is clear, however, that such observed changes in chemistry do not necessarily imply

25 chemical dynamics. Mixing across the boundary between the air masses may gen-

P. S. Anderson and W. D. Neff

erate real chemical interaction by bringing together otherwise separated trace gases, and we may expect the products to show a peak in concentration of the products at the boundary.

Transport may give the impression of reaction, by indicating a change in tracer con-
5 centration over time, whereas this may be due merely to the gradual (or possibly rapid) change of mass over the sample point. Perfect back trajectories would identify such a sudden switch in origin of the sample, such as from polar continental air to air originating over sea-ice.

Air masses are never as simple as implied by Fig. 2, being invariably three dimen-
10 sional structures. Air masses meet not at vertical boundaries, but with slopes dependent upon density and to some extent upon the relative velocity of the boundary with the surface. The horizontal scale of such boundaries or "fronts" can range from hundreds of kilometres for synoptic scale systems, to a few hundred metres for small scale drainage flows or "bores". In polar regions, where cooled air masses develop fre-
15 quently, small scale bores may be ubiquitous even within the otherwise homogenous boundary layers that form over ice shelves. Katabatic flow may be regarded as a continuous micro-front, transporting air from upstream underneath "local air". Over sea-ice, where variability in ice thickness, albedo and ice-coverage will lead to "thermal winds", effectively a drainage mechanism in a flat terrain caused by horizontal differences in air
20 density.

The sudden change in air mass associated with such a bore is shown schematically in Fig. 3; sampling of such a flow may result in the vary rapid time series variability, as seen in (Jones et al., 2006) where the micro-frontal system is observed in sodar backscatter images.

25 3.2   Vertical mixing

Mixing through the action of turbulence is the essence of the boundary layer. Although turbulence will be roughly isotropic, gradients of scalars such as trace gases will usually be largest in the vertical direction, and hence transport due to these gradients is

ACPD

7, 7625–7677, 2007

Boundary layer physics over snow and ice

P. S. Anderson and W. D. Neff

Title Page

Abstract	Introduction
Conclusions	References
Tables	Figures

◄◄ | ►►

◄ | ►

Back | Close

Full Screen / Esc

Printer-friendly Version

Interactive Discussion

EGU

predominantly towards or away from the surface.

3.2.1 Flux vs concentration

The study of any particular air chemistry species invariably starts with a time series of species concentration at a fixed height. The simplest representation of the time evolution of concentration is given by the following prognostic equation:

$$\frac{dC}{dt} = u\nabla C + \frac{\partial F}{\partial z} \tag{2}$$

This states that the change in concentration is the sum of the advective term and the flux divergence. The advective term encompasses an change in concentration, (∇C), in space being transported past the sample inlet by the wind, u. The vertical flux divergence causes an actual increase or decrease at some level. If the trace gas data available are limited to a single time series at one level, there is insufficient information to estimate the relative magnitude between advection and divergence in even this simplest of representations.

Most real air chemistry will involve active tracers, and hence there are additional loss/gain terms. Only by assuming horizontal homogeneity in C, such as may exist over a large physically homogenous ice shelf or ice cap, can ∇C be assumed small. In Anderson and Bauguitte (2006) this assumption allowed the loss terms to be estimated, by measuring dC/dt and estimating the flux using turbulence proxies (see below: Sect. 4.1: the neutral boundary layer).

To avoid the need to assume homogeneity, or to estimate better the loss terms for active tracers, the actual flux divergence should be measured, by making co-temporal measurements of concentration at two different heights, in conjunction with a measure of mixing efficiency. The flux is then given by:

$$F = K\frac{\partial C}{\partial z} \tag{3}$$

K is the diffusivity, a measure of the efficiency of the turbulent mixing. This equation may be understood in two ways.

- For a given flux (F known), increasing the mixing will reduce the concentration gradient.

- For a given gradient, ($\partial C/\partial z$ known), multiplying by K gives the flux.

Both of these concepts should be born in mind when designing trace gas flux measurements; for an expected flux, e.g. photo-genic NO_x, the largest "signal" to give $\partial C/\partial z$ will occur on days when K is small. Conversely, simply stating $\partial C\backslash\partial z$ data does not give any indication as to the fluxes, as K is also time dependent. K can be measured directly using sonic anemometry, (Neff et al., 2007) or estimated (Jones et al., 2001; Saiz-Lopez et al., 2007[2]).

3.2.2 Variable diffusivity with height, $K(z)$

Although mixing within the boundary layer is highly efficient, as discussed more fully below, the efficiency reduces as the surface is approached, eventually falling to molecular diffusive efficiencies at the ground. This variable diffusivity will tend to generate log-linear profiles of $C(z)$ near the surface when there is a flux of C in the vertical. More generally, a typical profile of $K(z)$ will show an increase with height to some point within the boundary layer and then decrease to zero at the top (where turbulence decreases to zero) (Stull, 1988).

3.2.3 Surface contact

Mixing occurs within the boundary layer, intermingling parcels of air from different places. Mixing also occurs at the surface in that air which make fleeting intimate con-

---

[2]Saiz-Lopez, A., Mahajan, A. S., Plane J. M. C., Anderson, P. S., Bauguitte, S. J.-B., Jones, A. E., et al.: On the vertical distribution of boundary layer halogens over coastal Antarctica, J. Geophys. Res.-Atmos., submitted, 2007.

Boundary layer physics over snow and ice

P. S. Anderson and W. D. Neff

tact with the ground is then mingle with overlying air. Knowledge of the efficiency of this surface contact is needed to understand, say, the importance of the catalytic effect of ice on the reactions. This surface contact may be vastly enhanced by two processes

  – Drifting or blowing snow

5 – Wave and wind pumping

Drifting and blowing snow has an effective surface are many orders of magnitude greater than a simple surface. Not only is the true surface in contact with the turbulent air all the greater, but the ice particles are better aspirated by continually falling through the air, and being subject to alternating air velocities.

10   Wave and wind pumping is the ventilation of the static but porous snow (firn) by the surface pressure field. Both of these topics are still open to study, and therefore beyond the scope of this paper.

3.2.4   Micro-scale mixing

When studying reaction rates between mixtures of liquids in flasks, the fluids are mixed
15 within the flask by mechanical means, often by a rotating lozenge shaped magnet. The spinning magnet generates a vortex which circulates the reagents by Ekman pumping, ensuring a homogenous mix of reagents. This mixing is necessary to ensure the time scales across the reaction vessel are dominated by the reaction rates, not by diffusion. If the rate is to be measured to better than a second, diffusion scales, L_D, must be less
20 than about 0.1 mm, from $L_D \sim \sqrt{(K_{mol}.t)}$ where K_{mol} is molecular diffusivity in $m^2 s^{-1}$. When reagents are closer together than this length, molecular diffusivity will be rapid enough to smooth out the mixture.

   Similarly, mixing at the micro-scale is also necessary within the air. Obviously the different reactants must be brought into proximity (within the same volume of air), but
25 also need to be mixed on the micro-scale. Such micro-scale mixing is inevitable with turbulence, due to the cascade of mixing scales from large to small to microscopic that

is inherent in the flow. At present, limitation due to the absence of micro-mixing is not seen as an issue in the community, but may be relevant under stratified conditions, where our assumptions of the turbulence cascade may break down.

4   Boundary layer types

The large scale structure of the boundary layer, and the subsequent efficiency for vertical mixing, depends primarily on the wind speed and the temperature structure. For certain cases there are additional constraints, such as the local slope of the surface or the up-wind terrain. We will describe the following broad boundary layer types:

- Neutral

- Convective

- Moderately stable over flat terrain

- Moderately stable over sloping terrain

Two other significant and identifiable "types" of polar boundary layer are the polynyal or Marginal Ice Zone (MIZ) boundary layer, and the complex stable boundary layer. The polynyal boundary layer occurs when cold stable air advects over warm open sea water, usually within sea-ice. The complex stable boundary layer occurs when stratification is sufficiently extreme to suppress wind shear generated turbulence; this type occurs over flat terrain such as ice shelves or closed pack-ice. Both types are of major interest to the polar air chemistry community, but their additional complexity and lack of suitable universal models preclude their discussion in this introductory paper.

EGU

4.1 The neutral boundary layer.

4.1.1 The Ekman layer

Air flow over the ground will form a turbulent region in the lowest tens to hundreds of metres above the surface through the action of drag induced wind shear. The turbulence is enhanced by convection, and suppressed by stable stratification; the neutral boundary layer is thus a suitable starting point from which to discuss the properties of the atmospheric boundary layer.

The turbulent intensity generally decreases with height, and a measure of the depth of the boundary layer is where turbulence tends to zero, or some small fraction of the surface value. Intensity is not an indication of mixing efficiency, however, which initially increases with height before decaying to zero again at the top of the boundary layer. If the potential temperature, $\theta(z)$, is constant with height (see Appendix A for a definition of θ) the profile is neutrally stratified and buoyancy plays no part in modifying either the mean flow or the turbulence. In an ideal case of flat, homogenous terrain, a static pressure field (which drives the upper level winds), and zero horizontal temperature gradients, the wind profile within the boundary layer should be expected to be described by Ekman's equations:

$$u = u_g \left(1 - e^{-\gamma z} \cos \gamma z\right)$$
$$v = u_g e^{-\gamma z} \sin \gamma z \tag{4}$$

where u_g is the free atmosphere wind speed (the geostrophic wind), z is height. u is the component of the wind parallel to the pressure contours, and hence parallel with the geostrophic wind, v is the orthogonal component. γ is a function of latitude and turbulent intensity formally described below, but at this point the interest of these equations from the polar chemistry perspective is that γ gives an estimate of boundary layer height, at least for neutral stratification. By noting that when $z=\pi/\gamma$, v must become zero, we can identify this height as the depth of the boundary layer. Below this level, the wind veers due to surface friction transported by turbulence, above this level, veer

is zero, and we can assume turbulence and hence mixing is zero. γ is therefore a useful scale, and is defined as

$$\gamma = \left(\frac{f}{2K}\right)^{1/2} \tag{5}$$

$f = 2\Omega\sin\phi$ is the Coriolis parameter, a measure of how much the earth's rotation affects large scale flow. Ω is the angular rotation of the earth, $= 2\pi$ radians per day, or 7.27×10^{-5} rad s^{-1} and ϕ is the latitude; hence f is known exactly for any given site.

K is the eddy viscosity or eddy diffusivity, with units of m^{2}s^{-1}. In Ekman's analysis, K is assumed to be constant with height, a major simplification and significant inaccuracy near the surface. K can be derived from turbulence measurements, and an approximation of K as a function of wind speed for snow is derived below. As an indication here, for a 5 ms^{-1} wind ($K \sim 2$ m^2 s^{-1}), at Halley (76° S, $f = 1.4\times10^{-4}$ s^{-1}), the Ekman derived boundary layer depth would be ~500 m. This is larger than generally observed at Halley during the winter, although not unknown in summer (h_z estimates from acoustic radar). This indicates that vertical stratification (i.e. buoyancy) can significantly affect the boundary layer at this site. One important aspect of the Ekman boundary layer is that there is a component of the flow nearest the surface toward lowest pressure whereas at the top of the boundary layer the flow matches the direction of the geostrophic wind.

For a clear and concise derivation of these equations, see Houghton (1986), pp. 129–130.

4.1.2 Surface layer diffusion

The eddy diffusivity, $K(z)$, is central to understanding both the boundary layer per se, and the vertical mixing within it. It can only be measured directly by sensitive in situ sensors (see sonic anemometers below), and hence much of boundary layer physics involves making parametric estimates of $K(z)$ based on more easily measured vari-

ables such as wind speed, surface radiation and, when stratification is significant, temperature profiles.

Fluxes of long lived tracers within a turbulent region are governed by the tracer gradient and the diffusivity. In a real boundary layer this diffusivity is a function of height, and similarity arguments suggest that near the surface $K(z)$ is given by

$$K(z) = 0.4zu_* \tag{6}$$

where 0.4 is the von Karman constant, z is height and u_* is the friction velocity. This lowest region of the boundary layer is termed the surface layer and is defined as the region where vertical fluxes (e.g. of momentum or heat) are virtually constant. The surface layer is typically the lowest 10%–20% of the full depth of the mixing layer.

u_* is related to the surface momentum fluxes by:

$$u_* = \left[\left(\overline{u'w'} \right)^2 + \left(\overline{v'w'} \right)^2 \right]^{1\!/2} \tag{7}$$

If the surface layer is, in fact, a "constant flux" layer, then u* can be measured at any height within it.

Equation (6) indicates that $K(z)$ tends to zero at z=0; at the surface there will be no diffusion. To avoid this physical unreality, the equation is assumed to hold down to a height where wind speed becomes zero, that is the roughness length, z_0. For snow, this roughness can be very small, e.g. 5×10^{-5} m over an ice shelf (King and Anderson, 1994). At these scales, $K(z_0)$ will be comparable with molecular diffusion, which implies a smooth transition from molecular dominated diffusion within the firm, to molecular diffusion within the atmosphere at z_0 , to turbulent diffusion aloft. Such simple surface layer theories allow, in principle, deduction of z_0 and the surface layer fluxes from high resolution temperature and wind profiles within the surface layer. These estimates hold well for the neutral and convective cases but are not as robust under stable stratification because turbulence does not achieve equilibrium with the mean flow in a simple manner.

Boundary layer physics over snow and ice

P. S. Anderson and
W. D. Neff

EGU

4.1.3 Surface Layer Diffusion with loss

The last form to consider under purely neutral stratification is leaking diffusion, where the 1-D version of the prognostic diffusion Eq. (2) includes a loss term:

$$\frac{dC}{dt} = \frac{d}{dz}\left(K\frac{dC}{dz}\right) - \frac{C}{\tau} \tag{8}$$

The first term on the right is the flux divergence formulated in terms of $K(z)$, and the second term is a loss, proportional to the local concentration, C, divided by a time constant, τ. This equation is explored for various scenarios in Anderson and Bauguitte (2006) for a surface trace gas source, comparing the equation solutions to CHABLIS measurements. The equation generates typical profiles of concentration, $C(z)$, such as shown in Fig. 4. An intuitive feel for the shape of these profiles is useful when estimating suitable sampling levels for trace gas flux measurements, in that using a lower sampling inlet within centimetres of the surface will give a larger concentration difference compared to, say at 4 m, but the expected curvature in $C(z)$ between the inlet tubes may become significant. The equation can be solved for diurnal variations in surface boundary conditions which generate non-stationary time series at a given height. This can be used to estimate the τ from measurements of $C(t)$ at a single level.

4.1.4 Correlation between h_z, u_* and C

A number of papers have noted an apparent anti-correlation between the near surface concentration of nitric acid (NO) and the depth of the boundary layer, h_z (Davis et al., 2004a; Neff et al., 2007). Such a correlation is explained in terms of containment size, in that a small h_z implies that the NO released into the boundary layer is trapped in a small volume, and therefore accumulates more rapidly leading to a longer lifetime and thus a non-linear growth in NO .(Davis et al., 2004a). There is also an observed correlation between h_z and u_* (Neff et al., 2007) in that more vigorous turbulence, reflected in u_*at the surface, implies a greater depth of mixing before turbulence is damped out,

Title Page

Abstract | Introduction

Conclusions | References

Tables | Figures

◄ | ►|

◄ | ►

Back | Close

Full Screen / Esc

Printer-friendly Version

Interactive Discussion

EGU

either by stratification or simple destruction of turbulence by viscous dissipation.

Given that the diffusivity *also* depends on u_*, in that large u_* implies large $K(z)$, rapid transport away from the surface will associate with low concentrations. That is, large u_* causes:

- Deep boundary layers.

- Low surface concentration.

As described in Neff et al. (2007) for stable boundary layers, h_z depends on both u_* and the background stability. While the magnitude of h_z can affect longer lived species such as NO, Anderson and Bauguitte (2006) argue that for a systems with short-lived species where

$$\frac{\tau u_*}{h_z} < 5 \tag{9}$$

the depth of the boundary layer has no effect on C at any level: i.e. loss terms dominate over diffusion.

4.2 The Convective Boundary Layer (CBL)

Convection occurs when the surface temperature exceeds that of the overlying air mass. Much of the following discussion will refer to potential temperature, θ, not actual temperature, T. The potential temperature accounts for adiabatic effects as a parcel is raised or lowered in height; when the atmosphere is vigorously stirred and buoyancy is zero, the change in pressure with height causes temperature to fall. Potential temperature adjusts for this effect, and a well mixed atmosphere has constant $\theta(z)$. For ease of reference , Appendix I provides the conversion equations to calculate potential temperature, $\theta(z)$, from measured temperature, $T(z)$, or temperature/pressure data, T,P: this latter conversion is useful when data are from radiosondes, which measure T and P only, and height must be derived.

The most obvious mechanism that generates a surface temperature excess is insolation, the absorption of shortwave radiation by the surface. Over snow this effect is minimized to some extent by the high albedo of the snow surface, and two other mechanisms may prevail: long-wave radiation imbalance and advection of cold air over a warmer surface.

Convection in the boundary layer is characterized by relatively thin plumes of rising air surrounded by the descending bulk of the air mass. The upper limit of the rising plume is governed by the rate of heating at the surface and the overall temperature structure of the atmosphere: when the rising plume comes into (potential) thermal equilibrium with the surrounding air, the buoyancy force becomes zero, and, following some overshooting due to inertia, the rising air parcel comes to rest.

For the air chemistry modeling perspective, convection modifies the boundary layer in the following ways:

- Vertical diffusion (mixing) is enhanced

- The boundary layer height (mixing depth) is generally deeper than for the neutral case.

- Upward diffusion (from the surface into the mixed layer) is more rapid than downward diffusion (top of boundary layer into the mixed layer)

These aspects are treated in detail elsewhere, e.g. in Nieuwstadt (1998) and Schumann (1989), but will be discussed briefly here. The energy available to be transported by the plumes is governed by the surface heat flux, and a scaling velocity, w_*, is derived from local surface parameters:

$$w_* = \left(\frac{g}{T_0} \langle w' \theta' \rangle_0 \, h_z \right)^{1/3} \tag{10}$$

where g/T_0, the buoyancy parameter, is the acceleration a parcel of air experiences for each degree Kelvin of excess temperature. $g = 9.81$, $T_0 =$ surface temperature in

Boundary layer physics over snow and ice

P. S. Anderson and W. D. Neff

EGU

Kelvin. $<w'\theta'>$ is the kinematic sensible heat flux as measured by eddy covariance, with units of m s^{-1} K. h_z is the height of the mixing layer.

In the absence of covariance measurements, $<w'\theta'>$ must be approximated from the surface energy balance:

$$\langle w'\theta' \rangle .\rho C_p + Rn + G(+H_\lambda) = 0 \tag{11}$$

where ρ is the air density and C_p is the specific heat at constant pressure = 1005 J kg^{-1} K^{-1}. Rn is the net radiation flux, and G the heat flux into the snow. If the surface is not melting, (< 0°C) G is usually small compared to Rn and in extremis can be neglected. Similarly, at cold temperatures, vapour pressures for water are small, and the latent heat flux, H_λ, can be neglected. On balance, it is best to measure $<w'\theta'>$ if possible.

During convection the top of the boundary layer is often clearly visible on acoustic radar (sodar) due to the strong temperature gradients often associated with the region (see Fig. 1 for typical convective profiles), hence the sodar data are highly desirable in order to get h_z.

There are two different diffusivities associated with the CBL, depending on the direction of diffusion (Nieuwstadt, 1998; Schumann, 1989). Bottom up diffusion is more efficient than top down due to the thinner plumes of ascending air rising more rapidly than the descending air. Figure 5 shows the two diffusion coefficients plotted on dimensionless axes. Height (y-axis) and diffusion (x-axis) are normalised using w_* and h_z: once these two scales are known, the form of the plots provide an estimate for the diffusion of tracer within the CBL.

The form of the two dispersion coefficients, K_b ("bottom up", i.e. suitable for tracer released at the surface) and K_t ("top down", i.e. suitable for tracer entrainment at h_z)

are:

$$K_b = 2.5 \left(1 - \frac{z}{h_z}\right) \left(\frac{z}{h_z}\right)^{3/2}$$
$$K_t = \left(\frac{z}{h_z}\right) \left(1 - \frac{z}{h_z}\right)^{3/2}$$

(12)

4.3 The moderately Stable Boundary Layer (SBL) over flat terrain.

The stable boundary layer is almost ubiquitous in polar regions, due to the combined
effects of the infra-red properties and albedo of the snow and low sun angle (or darkness). The low absolute humidity of the atmosphere and frequent cloud free conditions
also contribute to the net loss of radiation from the surface and the cooling of the atmosphere from below. The prevalence of the SBL in polar regions is unfortunate for the air
chemistry community; the physics of the SBL is still poorly understood (Mahrt, 1999).
Simple parametric schemes for the vertical diffusion profile are not valid, and various
non-local schemes are required to include flow history and other non-local mechanisms
such as waves. For the SBL, some level of micro-meteorological measurements is essential. There are a few situations where things are not so bleak: the weak SBL over
(very) flat terrain, and in certain cases where flow can be maintained at some minimum
level due to katabatic forces can be amendable to modeling such as the recent results
of Wang et al. (2007). However, measurement is required to estimate when conditions
are suitable for applying the limited understanding we do have of the SBL.

The CBL has an inherent negative feedback in the diffusion; if the bulk or mean $K(z)$
becomes to great, the heat is sucked from the ground too rapidly, reducing the over
temperature generating the convections. The reverse is true of the SBL. Stability is
initially generated by a surface cooler than the overlying air. $K(z)$ enables the air to
supply warmth to the surface. Stability acts to reduce turbulence, hence mixing and
hence $K(z)$. If $K(z)$ is reduced, less warmth reaches the ground, it cools more rapidly,
and increases the stability even more. The SBL has an inherent positive feedback,

Boundary layer physics over snow and ice

P. S. Anderson and
W. D. Neff

Title Page

Abstract | Introduction

Conclusions | References

Tables | Figures

◄ | ►

◄ | ►

Back | Close

Full Screen / Esc

Printer-friendly Version

Interactive Discussion

EGU

making it, at best, highly sensitive to forcing such as cloud cover or wind speed. In extreme cases, the SBL can become completely devoid of mixing in which case radiative flux divergences within the air and internal wave motions will dominate in the lowest layers of the atmosphere. This section reviews the techniques suitable for the SBL that is still well mixed, in that turbulence is still (relatively) active at all levels. The more extreme cases are discussed below.

A measure of stability is given by the Richardson Number, *Ri,* of which there are a variety of forms, but all aim to be measure of the balance between the generation and the absorption of turbulence in a stratified flow. In the simple SBL (i.e. ignoring complexities such as waves, orography), turbulence is generated by wind shear, as per the neutral boundary layer. Stratification suppresses turbulence by the forces of buoyancy; parcels of air moving vertically in a stably stratified flow will experience a restoring force to the motion. *Ri* is the ratio of these competing mechanisms:

$$Ri = \frac{g}{T} \frac{d\theta/dz}{\left(du/dz\right)^2} \tag{13}$$

The upper temperature gradient encompasses the buoyancy, the lower wind gradient the shear. *g* and *T* (absolute mean temperature) are included to make *Ri* dimensionless. Under neutral conditions, with no buoyancy, *Ri*=0. As stability increases, *Ri* increases.

Theoretical and wind tunnel studies indicated that if the flow has Ri>0.25, then turbulence should be suppressed, and the flow will be laminar. This magic number of 1/4 is often cited, but in the real world of environmental flows with large Reynolds numbers, such absolutes are not confirmed, and intermittent turbulence is still found in flows with mean *Ri* far in excess of 1/4.

Unlike the neutral and convective boundary layer, there are as yet no simple prognostic equations for the diffusivity aloft, nor the depth of the mixing layer. There is an inherent complexity in the flow, which can be captured by considering a very slightly

Boundary layer physics over snow and ice

P. S. Anderson and W. D. Neff

stable boundary layer, where the temperature gradient is (unrealistically) constant. Figure 6 (temperature) and Fig. 7 (diffusivity) show how such a model is expected to evolve if the surface and upper level temperatures are fixed. Mixing near the surface reduces the temperature gradient, whilst reduced mixing at mid-levels allows the development of an "inversion". The strong gradients in the inversion enhance the stability, and suppress mixing further. The result is a boundary layer potential temperature profile, $\theta(z)$, with positive curvature, that is $d^2\theta/dz^2 > 0$; the $\theta(z)$ is concave to the right. This is for an idealized case where there is no net surface cooling; even so, there are significant differences between models for this most simplified of stable cases. For a discription of the comparison, see Cuxart et al. (2006), Holtslag (2006), Kerstein and Wunsch (2006) and Steeneveld et al. (2006). Compare these figures with observed profiles, where surface cooling does occur. Figures 8 and 9 are tethersonde profiles and sodar echogramme recorded at Halley during the winter of 2003. The rapidity of the cooling results in a profile where $d^2\theta/dz^2$ is negative, that is, the profile is concave to the left. Such $\theta(z)$ profiles are ubiquitous at Halley where the absence of slope precludes the onset of drainage flow. Drainage, or katabatic flow, acts to limit the magnitude of the temperature gradient by maintaining the strength of the near surface turbulence.

Real SBLs are often complex, in that the variation of $K(z)$ aloft affects the temperature gradient itself. Near the surface, Ri tends to small values (except under near calm wind conditions), and the diffusion is relatively well behaved. Aloft, however, the wind shear reduces, whilst the temperature gradients remain relatively constant; hence Ri generally increases with height until turbulent activity is affected. Feedback between stability and diffusion is then highly non-linear, and the predictive ability of boundary layer theory becomes poor. For a more thorough overview of the difficulties in parameterising the stable boundary layer, see Mahrt (1999), Mahrt and Vickers (2006), Vickers and Mahrt (2004), Zilitinkevich and Baklanov (2002) and Zilitinkevich et al. (2002).

What then can be done to calculate the diffusion profile, $K(z)$? Two options are available, neither ideal. First is to use a 1-D SBL model which can produce $K(z)$ as a diagnostic. Such models are constrained by measurable boundary conditions, the

Boundary layer physics over snow and ice

P. S. Anderson and W. D. Neff

most important being wind speed and snow surface temperature, T_s. If T_s is left free, such models for flat terrain tend to dramatically over or under estimate the temperature gradients, due to internal sensitivity of these models. At present, 1-D SBL models appear to be very poor at reproducing measured temperature profiles. There is a lack
5   of in situ measurements of $K(z)$, but the failure of the temperature validation implies there will be a similar discrepancy between model and real diffusivity profile.

The second approach is to rely on measurement, and is it the SBL which most benefits from the sodar and sonic anemometer data. Sodar images will indicate when the SBL is well behaved and therefore suitable for thorough analysis, and thence also indi-
10   cate the depth of the mixing layer. The sonic anemometry assists in constraining and testing the validity of model diagnostics. For flat terrain, there are frequently events where the sodar echo signature exhibits complex structure aloft, this being prevalent under moderate to calm wind conditions. With slightly higher winds, the sodar data implies a well ordered SBL, with a clear measurable upper limit. It will be these oc-
15   casions when air chemistry modeling, based on some prescribed $K(z)$ profile, will be most valid.

4.4   The stable SBL over sloping terrain

Much of the interior of Antarctica is characterized by small terrain slopes ($\sim$0.001 to 0.002), strong wintertime temperature inversions and relatively weak summertime in-
20   versions. Much of our understanding of the micrometeorology of this region and its linkages to the large scale circulation has come from studies at the South Pole (Neff, 1980, 1999; Neff et al., 2007). In very general terms, radiative cooling for the surface, which prevails even in summer except for overcast periods (Carroll, 1984), creates a surface temperature inversion overlying the sloping ice surface. This creates a downs-
25   lope pressure gradient which under weak synoptic forcing results in a very constant Ekman layer flow. In addition, the large-scale pressure gradient is often also downslope leading to persistent downslope winds even in summer. Because there is no diurnal cycle, this is a unique location for the study of stable boundary layers modulated

primarily by only synoptic scale weather sytems. As noted by Neff (1999), the winds aloft are typically bimodal leading to an alternation between an upslope and downslope oriented large scale pressure gradient. When this pressure gradient is oriented upslope, it opposes that created by the effect of the inversion overlying the sloped surface
5   and winds become very light but typically non-zero. Because such conditions typically occur with clear skies, very strong inversions also form creating a contradiction with the traditional conceptual picture of strong inversions resulting in downslope flows. When the winds aloft reverse, the pressure gradient becomes downslope with stronger surface winds, increased mixing, weaker inversions and deeper boundary layers. These
10 conditions usually occur with increases in cloudiness and thus radiative cooling of the surface is of less influence.

Recent interest in this meteorological environment has been stimulated by observations of very high nitric oxide concentrations at the South Pole in 1998 and 2000 (Davis et al., 2001) and thought to be due to the non-linear growth in NO associated
15 primarily with very shallow boundary layers (Davis et al., 2004a). A follow-on study in 2003 added a number of measurements to document the boundary layer properties and vertical profile characteristics for NO and O_3 (Helmig et al., 2007a; Helmig et al., 2007b; Neff et al., 2007). Together with sonic anemometer turbulence measurements and data from a 22-m tower, this experiment provided a unique opportunity for relating
20 surface chemistry to the slowly changing meteorology of a stable boundary layer. Key findings from this study include

- Both boundary depth and NO depend on u_*: i.e. a small friction velocity results in limited mixing and high NO values.

- Simple boundary layer depth scaling results, using u_* and stability, agree well with
25   sodar-observed mixing layer depths.

- Estimated vertical diffusion times to depths of 30 m are on the order of nine hours under light wind conditions, sufficient to allow non-linear NO chemistry to be ac-

tivated which occurs with NO concentrations in excess of 200 pptv, when NO increases result in OH reductions: (Davis et al., 2004a).

– Observed sodar mixing layer depths agreed well with those calculated from a 1-D model (Wang et al., 2007).

5 – The use of a sodar to provide consistent mixing-layer depth estimates allowed identification of anomalous periods that could only be explained by increased fluxes of NO from the snow.

5 Measurement techniques, instruments and field studies

A boundary layer air chemistry campaign will generally benefit from some level of
10 micro-meteorological data, in order to understand local mixing and transport. Instrumentation and deployment costs will limit the availability of these data. This section describes typical micro-meteorological field instrumentation which would benefit a major air chemistry campaign, roughly in order of increasing cost and usefulness.

5.1 Automatic Weather Stations (AWS)

15 A typical AWS will measure wind speed and direction, temperature, humidity and pressure near the surface. Additional instruments are often deployed, such as an additional temperature sensor, radiometers and snow depth sensors. Commercial units tend to come equipped with solar panels for power and telemetry, to send data back to the user. In polar environments, these units must be modified, or custom designs used,
20 to cope with the harsher environment, lower temperatures, lack of communication infrastructure and long polar nights. A useful guide to suitable AWS for polar work is provided by (Oerlemans and Tijm-Reijmer, 2004). This manual discusses the present optimum instrument designs to deploy over snow, such as preferring propeller-vane wind instruments over cup anemometers.

The AWS will only provide limited information on the structure of the boundary layer, the data being used as if standard meteorological data were available (Jacobi et al., 2000; Jones et al., 2001). u_* can be estimated from wind speed, assuming neutral stratification and a known or estimated roughness length.

5   A temperature measurement at a second level (>2 m vertical from the first sensor) identifies when strong, stable stratification exists. This stratification will modify the vertical mixing from the surface, but this can be estimated along with the down-welling sensible heat flux (van den Broeke et al., 2005). Unfortunately, convection cannot be distinguished from neutral stratification by a pair of temperature sensors, due to inso-
10   lation errors on the sensors, and the much smaller temperature gradients associated with convection.

Wind direction will be useful in complex terrain, such as mountains, but re-analysis data will be just as accurate elsewhere. In terms of understanding the dynamics of the air chemistry, the AWS is better than nothing, but only just. Figure 10 shows a typical
15   polar AWS deployed in Coats Land.

5.2   Radiometers

Micro-meteorological radiometers are broadband instruments. The "J-Spectrometer" radiometer is more a specialist chemistry instrument, and not discussed here.

Radiometers may be added to the standard AWS equipment, but due to power con-
20   straints such sensors are generally un-aspirated, and can therefore be adversely affected by rime-icing. Better data can be obtained using aspiration over the domes, which maintains the optics. Aspiration, however, requires significant power, only available in summer (photovoltaic) or by wind turbine or station generator. A good set of upward and downward longwave and short wave radiometer readings can give in-
25   formation on net radiative cooling or warming, cloud cover (by comparing long-wave readings), insolation and albedo. Figure 11 shows the four component CNR1 radiation unit, typically used on AWS, where no heating or aspiration power is available to reduce icing.

5.3 The profile mast

Over snow/ice, masts >30 m are difficult to maintain, and masts much below 10 m fall into the AWS category. A "profile mast" refers to 20–30 m height, and rigged with instruments arranged with logarithmic vertical spacing. Standard observations are
5 winds and temperature, aimed at measuring the gradients, that is the near surface wind shear and lapse rate. Measuring gradients requires a higher level of accuracy from the equipment than from an AWS, and polar profile masts invariably have aspirated temperature/humidity sensors, and require frequent observations to check for icing. Figure 12 shows the 32 m Instrumented Clean Air Sector (ICAS) mast at Halley,
10 Antarctica, located 50 m from the Clean Air Sector Laboratory (CASLab).

5.4 Sonic anemometers/thermometers

The de facto boundary layer micro-meteorological instrument is the sonic turbulence sensor or sonic anemometer/thermometer. This instrument measures wind and temperature fluctuations directly by measuring the time of flight of ultra-sound pulses. By
15 calculating the covariance of the vertical wind fluctuations, w', with other wind vectors (u' and v'), or with fluctuations of scalars such as temperature, H_2O or CO_2, the flux of momentum, heat, moisture and CO_2 respectively can be measured directly. The limitation to this technique is the need for a "fast" response sensor, typically 40 Hz or better. At present, for instance, there is no fast response NO_x sensor. However, fast re-
20 sponse O_3 sensors are under development and show promise (Detlev Helmig, private communication).
    Sonic anemometers require a significant level of understanding to ensure that the processed data are reliable. They are sensitive to a number of deployment effects, such as tilting or mast shadow, and require corrections to compensate for flow distortion
25 around the sensor as well as other effects. Lee et al. (2004) is an essential guide to the present state of the art of sonic anemometer data analysis. The alternative is to collaborate with a micro-meteorological group with a number of years of experience

with these instruments.

Sonic anemometers require significant power compared to AWS and radiometer, and again tend to be used either in summer only (with photovoltaics) or use station power. The instruments can be operated autonomously, but are sensitive to icing, hence require heated transducers. One sonic at two metres elevation can make a fair estimate of vertical transport by measuring $u*$ directly, and under katabatic conditions, estimate boundary layer depth (Neff et al., 2007) as well as giving wind speed, direction and temperature. The data can be logged at their raw output rate (typically 40 Hz) and the fluxes calculated afterwards, or some units calculate these fluxes and means. Putting sonics at various heights on a profile mast enhances the value of the data, partly as a check on data quality, but also by enabling boundary layer depth to be estimated by extrapolation. Figure 12 shows the ICAS mast with three sonic anemometers deployed. These units have sensor heating to reduce icing difficulties.

5.5   Acoustic radar or sodar

The structure of the near surface atmosphere can be qualitatively visualized using acoustic radars (Neff and Coulter, 1985). Sound will scatter from temperature inhomogeneities in the atmosphere, generated by wind shear acting on the temperature gradient under stable conditions or by convective elements rising from a warmer surface and mixing into the ambient fluid. Interpretation of the echo images is non-trivial, but the instrument has the ability to detect the upper level of the near surface mixing directly. Be aware that there are two types of sodar: backscatter and wind profiling. The latter is invariably provided by the commercial sector, who market the units as a replacement for expensive profile masts. The boundary layer and air chemistry research community are becoming more familiar with the original backscatter only system, which provide profiles of the temperature structure function, often referred to as $C_T^2(z)$. These sodars are relatively simple but invariably a non-commercial, in-house unit. These units are tuned to provide high resolution in the vertical, with one metre being typical, and under suitable conditions resolve the C_T^2 mixing depth to high accuracy, as well as provide in-

dications of internal boundary layer structure (Anderson, 2003; Culf, 1989). Standard sodars provide echo data from 20 m above the surface to around 1000 m, whilst mini-sodars work from 1 m to 200 m. They can operate autonomously given suitable care with the design and a robust power system (Anderson et al., 2005). Figure 13 shows the sodar used to assist interpretation of the CHABLIS data (Jones et al., 2006).

5.6 Balloon sondes (RAWINsonde)

The free flight balloon with meteorological instrument package will provide limited immediate data for use in air chemistry analysis, but, if the data are linked to the global analysis data centres (i.e. weather forecasting) the data will enhance the product in the locality of the field study. Meteorological balloon sonde systems are invariably commercial. Chemical balloon profiling is expensive, and geared for stratospheric studies, notwithstanding the analysis by Tarasick and Bottenheim (2002).

5.7 Tethersondes

The tethered sonde system, whereby an instrument package is taken aloft and subsequently recovered, is well suited to boundary layer air chemistry studies. With recovery virtually guaranteed, custom designed or bespoke sondes can be used, with on board logging to eliminate the need for a costly, complex and battery hungry transmitter. Simple filter sampling can be achieved using a relatively rapid ascent of the sonde followed by a period at constant altitude (Rankin and Wolff, 2002). In general, two (or more) sondes are flown in tandem, one for the meteorological profiles, one for the air chemistry sampling. Recent advances associated with the ANTCI program have revealed the value of balloon profiling for NO and O_3 (Helmig et al., 2007a; Helmig et al., 2007b). In the case of NO profiling, sampling is through a long tube and the delay in the line is a required correction.

The lifting platform can be either blimp or kite, depending on wind conditions and logistics and to some extent, expected temperature. Kites are less susceptible to micro-

damage from cold temperature effects on the material, and are more portable for field work. Blimps work in lower wind speeds, and can be flown with simpler winch systems, due to the lower line tensions required for lifting the same mass of sonde. They do require a significant helium source, reducing their suitability for remote operations.

5.8 Aircraft: manned and unmanned

A history and description of the state-of-the art of instrumented, piloted aircraft is beyond the scope of this paper, suffice to say that they are expensive but, until recently, provided unique area averaged data in a short time. This ability to sample over large areas, plus the means to sample away from a field station, will soon be achievable using robotic airplanes, or Unmanned Aerial Vehicles (UAVs). UAVs are controlled by on-board avionic and should not be seen as "radio controlled". They are given a programmed flight plan of way points, and the avionics then control the mission, including landing. Recent advances in miniaturisation of both avionics and GPS receivers allow small UAVs to be an affordable solution to making non-local measurements. Furthermore, advances in battery technology allow in excess of one hour duration of purely electric aircraft, ideal for air chemistry sampling. Figure 14 shows a montage of the Mavionics T200 overlaid on an ice-shelf image, to give an idea of the state of things to come. These units will fly at Halley, Antarctica during the winter of 2007.

5.9 Remote sensing

The atmospheric boundary layer is poorly understood, in part due to the limited use to which satellite data can be put to probe the atmosphere close to the ground; ABL studies require in situ measurements and suffer from the resulting lack of spatial information. One major exception is the retrieval of surface temperatures from infra-red imagery, assuming no cloud cover. The visualisation of extreme mixing within the ABL due to, say, strong katabatic flow is also possible, as shown in Bromwich et al. (1992) but vertical profiles, fluxes or upper boundary layer mixing cannot, as yet, be measured

ACPD

7, 7625–7677, 2007

Boundary layer physics over snow and ice

P. S. Anderson and W. D. Neff

Title Page

Abstract | Introduction

Conclusions | References

Tables | Figures

◄ | ►

◄ | ►

Back | Close

Full Screen / Esc

Printer-friendly Version

Interactive Discussion

EGU

by these techniques.

6 Summary

The physics of the boundary layer is of growing interest to the air chemistry and snow chemistry community. Despite the development of 1-D ABL chemistry models (Saiz-Lopez et al., 2007[2]), which are extensions of existing physical ABL models, a knowledge of the typical behaviour and known failings of such physical ABL models is beneficial to the community. Invariably, such models benefit from additional constraint derived from in situ measurements of the micro-meteorology. This paper has provided the main conceptual principals underlying ABL theory and associated models, and provides examples of useful micro-meteorological equipment to augment polar atmospheric air chemistry campaigns.

Appendix A

Useful equations

For the derivation and a clear discussion of how to use these equations refer to (Stull, 2000) where these forms are presented in difference notation, not as true integrals, which is most appropriate for working with digitised (finite step) data.

Ideal Gas Law: relates pressure, temperature and volume of a gas.

$$P = \rho \mathfrak{R}_d T \tag{A1}$$

Where P is the pressure in Pa, ρ is density in $kg\,m^{-3}$, T the absolute temperature in K, and R_d is the gas constant, $= 287.053\,J\,K^{-1}\,kg^{-1}$.

Boundary layer physics over snow and ice

P. S. Anderson and W. D. Neff

Hydrostatic Equation: gives the change in pressure with height if the density of the air is known.

$$\frac{\Delta P}{\Delta z} = -\rho g \tag{A2}$$

ΔP is change in pressure in Pa, Δz is change is height. ρ is density in kg m^{-3}, g is acceleration due to gravity = $9.81\,\text{ms}^{-2}$

The Hypsometric Equation. A combination of the ideal gas law and the hydrostatic equation, gives the change in height associated with a change in pressure for a given (mean) temperature

$$z_2 - z_1 = aT \ln\left(\frac{P_1}{P_2}\right) \tag{A3}$$

where z_1 and z_2 are heights, P_1 and P_2 the respective pressures, and T the mean absolute temperature between these heights. $a = R_d/g = 29.3\,\text{m K}^{-1}$.

Potential Temperature Conversion from Pressure.

If the temperature is know as a function of pressure, for instance in a radiosonde profile,

$$\theta = T\left(\frac{P_0}{P}\right)^{\Re_d/C_p} \tag{A4}$$

where P_0 is the pressure at the surface (or some reference pressure e.g. 1000 hPa), and C_p is the specific heat at constant pressure = $1005\,\text{J kg}^{-1}\,\text{K}^{-1}$ (assumes dry air which is reasonable for most polar temperatures).

Potential Temperature Conversion from Height

To calculate the true potential temperature

If only a temperature profile, $T(z)$ is known, the calculation of potential temperature first requires calculation of the respective pressure "profile", $P(z)$. Firstly, the hypsometric equation is used to calculate the small difference in pressure between readings:

$$P_{i+1} = P_i e^{\frac{z_1 - z_2}{aT}} \tag{A5}$$

Boundary layer physics over snow and ice

P. S. Anderson and W. D. Neff

Hence, starting at the ground with P_0, calculate P_1, the pressure at the next level up, using mean T between levels. Repeat for all levels to get $P(z)$. Potential temperature conversion is then calculated from pressure.

References

5 Anderson, P. S.: Fine-scale structure observed in a stable atmospheric boundary layer by Sodar and kite-borne tethersonde, Boundary-Layer Meteorol., 107(2), 323–351, 2003.

Anderson, P. S. and Bauguitte, S.: Behaviour of Tracer Diffusion in Simple Atmospheric Boundary Layer Models, Atmos. Chem. Phys., 6, 13 111–13 138, 2006.

Anderson, P. S., Ladkin, R. S., and Renfrew, I. A.: An autonomous Doppler sodar wind profiling
10 system, J. Atmos. Oceanic Technol., 22(9), 1309–1325, 2005.

Bottenheim, J. W. and Chan, E. A.: trajectory study into the origin of spring time Arctic boundary layer ozone depletion, J. Geophys. Res.-Atmos., 111(D19), D19301, doi:10.1029/2006JD007055, 2006.

Bromwich, D. H., Carrascoa, J. F., and Stearns, C. R.: Satellite Observations of Katabatic-Wind
15 Propagation for Great Distances across the Ross Ice Shelf, Monthly Weather Rev., 120(9), 1940–1949, 1992.

Carroll, J. J.: On The Determinants Of The Near-Surface Temperature Regime On The South Polar Plateau, 89(ND3), 4941–4952, 1984.

Culf, A. D.: Acoustic Sounding of the Atmospheric Boundary Layer at Halley, Antarctica, Antarc-
20 tic Sci., 1, 363–372, 1989.

Cuxart, J., Holtslag, A. A. M., Beare, R. J., Bazile, E., Beljaars, A., Cheng, A., et al.: Single-column model intercomparison for a stably stratified atmospheric boundary layer, Boundary-Layer Meteorol., 118(2), 273–303, 2006.

Davis, D., Chen, G., Buhr, M., Crawford, J., Lenschow, D., Lefer, B., et al.: South Pole NOx
25 chemistry: an assessment of factors controlling variability and absolute levels, Atmos. Environ., 38(32), 5375–5388, 2004a.

Davis, D., Eisele, F., Chen, G., Crawford, J., Huey, G., Tanner, D., et al.: An overview of ISCAT 2000, Atmos. Environ., 38(32), 5363–5373, 2004b.

Davis, D., Nowak, J. B., Chen, G., Buhr, M., Arimoto, R., Hogan, A., et al.: Unexpected high
30 levels of NO observed at South Pole, Geophys. Res. Lett., 28(19), 3625–3628, 2001.

Boundary layer physics over snow and ice

P. S. Anderson and W. D. Neff

Title Page

Abstract	Introduction
Conclusions	References
Tables	Figures

|◄ | ►|

◄ | ►

Back | Close

Full Screen / Esc

Printer-friendly Version

Interactive Discussion

EGU

Ekman, V. W.: On the Influence of the Earth's Rotation on Ocean-Currents. Arkiv For Matematik, Atronomi OCH Fysik, Band 2(No 11), 1–53, 1905.

Helmig, D., Johnson, B., Oltmans, S. J., Neff, W. D., Eisele, F., and Davis, D.: Elevated ozone in the boundary layer at the South Pole, Atmos. Environ., doi:10.1016/j.atmosenv.2006.12.032, 2007a.

Helmig, D., Warshawsky, M., Johnson, B., Buhr, M., Eisele, F. and Davis, D. Nitric oxide in the boundary layer at the South Pole during the 2003 Antarctic Tropospheric Chemistry Investigation, Atmos. Environ., doi:10.1016/j.atmosenv.2007.03.061, 2007b.

Holtslag, B.: Preface – GEWEX atmospheric boundary-layer study (GABLS) on stable boundary layers, Boundary-Layer Meteorol., 118(2), 243–246, 2006.

Houghton, J. T.: The Physics of Atmospheres (Second Edition ed.): Cambridge University Press, 1986.

Jacobi, H. W., Weller, R., Jones, A. E., Anderson, P. S., and Schrems, O.: Peroxyacetyl nitrate (PAN) concentrations in the Antarctic troposphere measured during the photochemical experiment at Neumayer (PEAN'99), Atmos. Environ., 34(29–30), 5235–5247, 2000.

Jones, A. E., Anderson, P. S., Wolff, E. W., Turner, J., Rankin, A. M., and Colwell, S. R.: A role for newly forming sea ice in springtime polar tropospheric ozone loss? Observational evidence from Halley station, Antarctica, J. Geophys. Res.-Atmos., 111(D8), D08306, doi:10.1029/2005JD006566, 2006.

Jones, A. E., Weller, R., Anderson, P. S., Jacobi, H. W., Wolff, E. W., Schrems, O., et al.: Measurements of NOx emissions from the Antarctic snowpack, Geophys. Res. Lett., 28(8), 1499–1502, 2001.

Kahl, J. D.: Characteristics Of The Low-Level Temperature Inversion Along The Alaskan Arctic Coast, Int. J. Climatol., 10(5), 537–548, 1990.

Kerstein, A. R. and Wunsch, S.: Simulation of a stably stratified atmospheric boundary layer using one-dimensional turbulence, Boundary-Layer Meteorol., 118(2), 325–356, 2006.

King, J. C. and Anderson, P. S.: Heat and Water-Vapor Fluxes and Scalar Roughness Lengths over an Antarctic Ice Shelf, Boundary-Layer Meteorol., 69(1–2), 101–121, 1994.

Lee, X., Massman, W., and Law, B.: Handbook of Micrometeorology: Kluwer Academic Publishers, Dordrecht, 2004.

Mahrt, L.: Stratified atmospheric boundary layers. Boundary-Layer Meteorology, 90(3), 375–396, 1999.

Mahrt, L. and Vickers, D.: Extremely weak mixing in stable conditions, Boundary-Layer Meteo-

rol., 119(1), 19–39, 2006.

Neff, W. D.: Boundary-Layer Research at South-Pole Station Using Acoustic Remote-Sensing, Antarctic J. United States, 13(4), 179–181, 1978.

Neff, W. D.: An observational and numerical study of the atmospheric boundary layer overlying
5   the east Antarctic ice sheet. Unpublished PhD, University of Colorado, Boulder, 1980.

Neff, W. D.: Decadal time scale trends and variability in the tropospheric circulation over the South Pole, J. Geophys. Res.-Atmos., 104(D22), 27 217–27 251, 1999.

Neff, W. D. and Coulter, R. L.: Acoustic Remote Sensing, in: Probing the Atmospheric Boundary Layer (pp. 201-236), edited by: Lenshow, D. H., Boston: American Meteorological Society,
10   1985.

Neff, W. D., Helmig, D., Grachev, A., and Davis, D.: A study of boundary Layer behavior associated with high NO concentrations at the South Pole using a minisodar, tethered balloon, and sonic anemometer, Atmos. Environ., doi:10.1016/j.atmosenv.2007.01.033, 2007.

Nieuwstadt, F. T. M.: Review of diffusion processes in the convective boundary layer, in: Buoy-
15   ant Convection in Geophysical Flows, edited by: Plate, E. J., 371–399, 1998

Oerlemans, J. and Tijm-Reijmer, C. H.: Automatic Weather Stations on Glaciers: Institute for Marine and Atmospheric Research Utrecht, Utrecht University, The Netherlands., 2004

Oltmans, S. J.: Surface Ozone Measurements In Clean-Air, J. Geophys. Res.-Oceans Atmos., 86(NC2), 1174–1180, 1981

20   Prandtl, L.: Verhandlungen des dritten internationalen Mathematiker-Kongresses in Hiedelberg 1904, In A., K. (Ed.) (pp. 484). Teubner, Leipzig, Germany, 1905.

Rankin, A. M. and Wolff, E. W.: Aerosol Profiling Using a Tethered Balloon in Coastal Antarctica, J. Atmos. Oceanic Technol., 19(12), 1978–1985, 2002.

Schnell, R. C., Barry, R. G., Miles, M. W., Andreas, E. L., Radke, L. F., Brock, C. A., et al.: Lidar
25   Detection Of Leads In Arctic Sea Ice. Nature, 339(6225), 530–532, 1989.

Schumann, U.: Large-eddy simulation of turbulent diffusion with chemical reactions in the convective boundary layer, Atmos. Environ., 23, 1713–1727, 1989.

Serreze, M. C., Maslanik, J. A., Rehder, M. C., Schnell, R. C., Kahl, J. D., and Andreas, E. L.: Theoretical Heights Of Buoyant Convection Above Open Leads In The Winter Arctic Pack
30   Ice Cover, J. Geophys. Res.-Oceans, 97(C6), 9411–9422, 1992.

Shepson, P., Matrai, P., Barrie, L., and Bottenheim, J. W.: Ocean-Atmosphere-Sea Ice-Snowpack Interactions in the Arctic and Global Change. EOS, 84(36), 349, 2003.

Steeneveld, G. J., Van de Wiel, B. J. H., and Holtslag, A. A. M.: Modelling the arctic stable

boundary layer and its coupling to the surface, Boundary-Layer Meteorol., 118(2), 357–378, 2006.

Stull, R. B.: An Introduction to Boundary Layer Meteorology. Dordrecht: Kluwer Academic Publishers, Dordrecht, 1988.

5 Stull, R. B. Meteorology for Scientists and Engineers (Second Edition ed.): Gary Garlson, 2000.

Tarasick, D. W. and Bottenheim, J. W. Surface ozone depletion episodes in the Arctic and Antarctic from historical ozonesonde records, Atmos. Chem. Phys., 2, 197–205, 2002, http://www.atmos-chem-phys.net/2/197/2002/.

10 van den Broeke, M. R., van As, D., Reijmer, C. H., and van de Wal, R.: Sensible heat exchange at the Antarctic snow surface: a study with automatic weather stations, Int. J. Climatol., 25(8), 1081–1101. 2005

Vickers, D. and Mahrt, L.: Evaluating formulations of stable boundary layer height, J. Appl. Meteorol., 43(11), 1736–1749, 2004.

15 Wang, Y., Choi, Y., Zeng, T., Davis, D., Buhr, M., Huey, G., et al.: Assessing the photochemical impact of snow NOx emissions over Antarctica during ANTCI 2003, Atmos. Environ., doi: 10.1016/j.atmosenv.2007.01.056, 2007.

Zilitinkevich, S. and Baklanov, A. Calculation of the height of the stable boundary layer in practical applications, Boundary-Layer Meteorol., 105(3), 389–409, 2002.

20 Zilitinkevich, S., Baklanov, A., Rost, J., Smedman, A. S., Lykosov, V., and Calanca, P.: Diagnostic and prognostic equations for the depth of the stably stratified Ekman boundary layer, Q. J. R. Meteorol. Soc., 128(579), 25–46, 2002

Boundary layer physics over snow and ice

P. S. Anderson and W. D. Neff

Title Page

Abstract | Introduction

Conclusions | References

Tables | Figures

◄ | ►

◄ | ►

Back | Close

Full Screen / Esc

Printer-friendly Version

Interactive Discussion

EGU
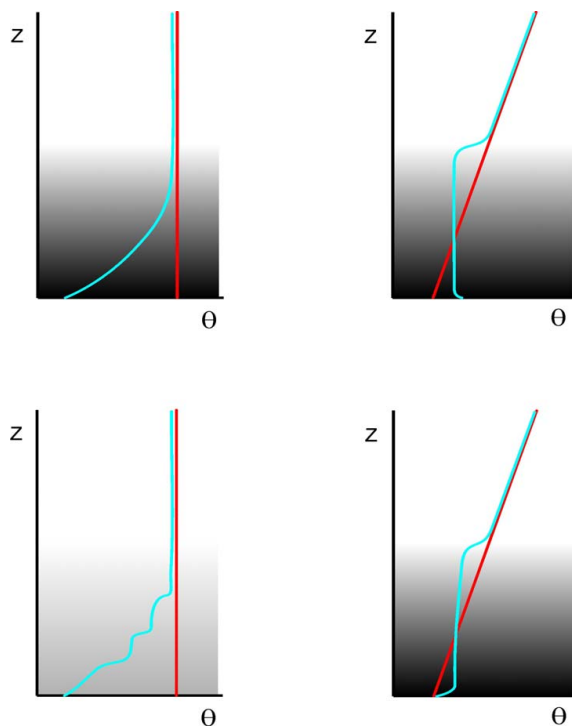
Fig. 1. Idealised initial temperature profiles (red) and their evolution (blue) within different boundary layer types. **(a)** Isothermal layer being cooled from below. **(b)** stable layer being mixed by convection, **(c)** isothermal layer with rapid cooling leading to complex structure and **(d)** "polynyal"; re-cooling of a stable layer following a convective episode.
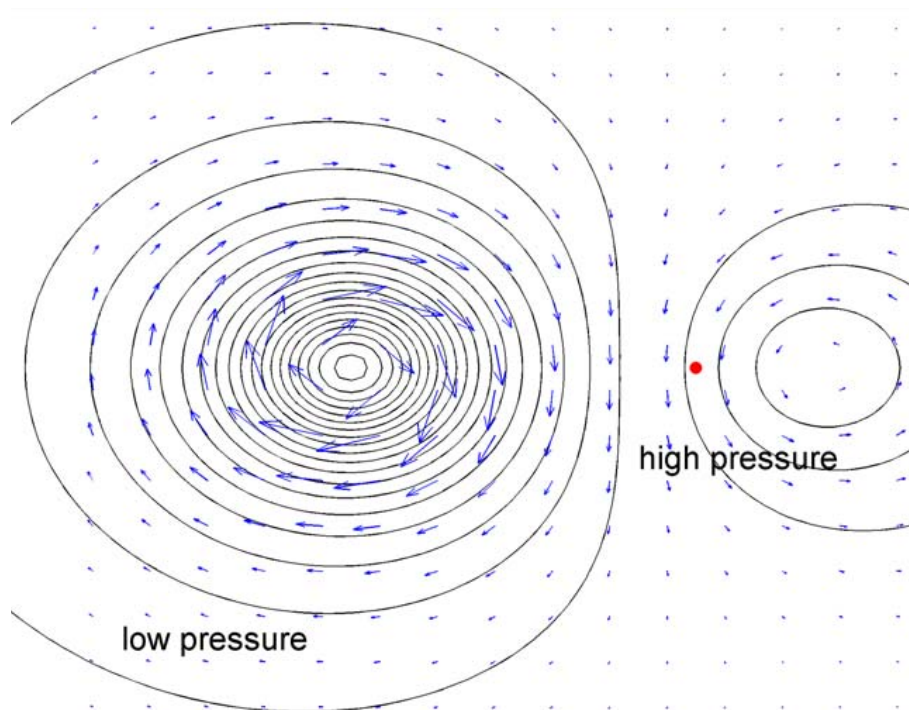
Fig. 2. Idealised synoptic flow as viewed from above, indicating possible sensitivity of back trajectory calculations to small changes in the synoptic wind field. The red dot is a possible sample position which would be exposed to a different air mass should the pressure systems shift slightly to the right, with no associated significant change in wind direction. NB, flow is for southern hemisphere.
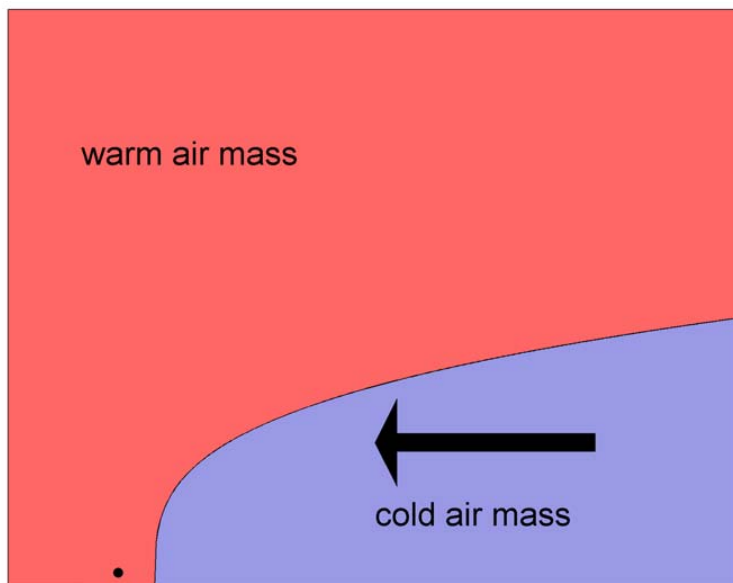
Fig. 3. Schematic of a frontal or bore system seen from the side. As the colder air slowly passes over the field site (small dot), very rapid changes in the tracer signature may be observed.

EGU
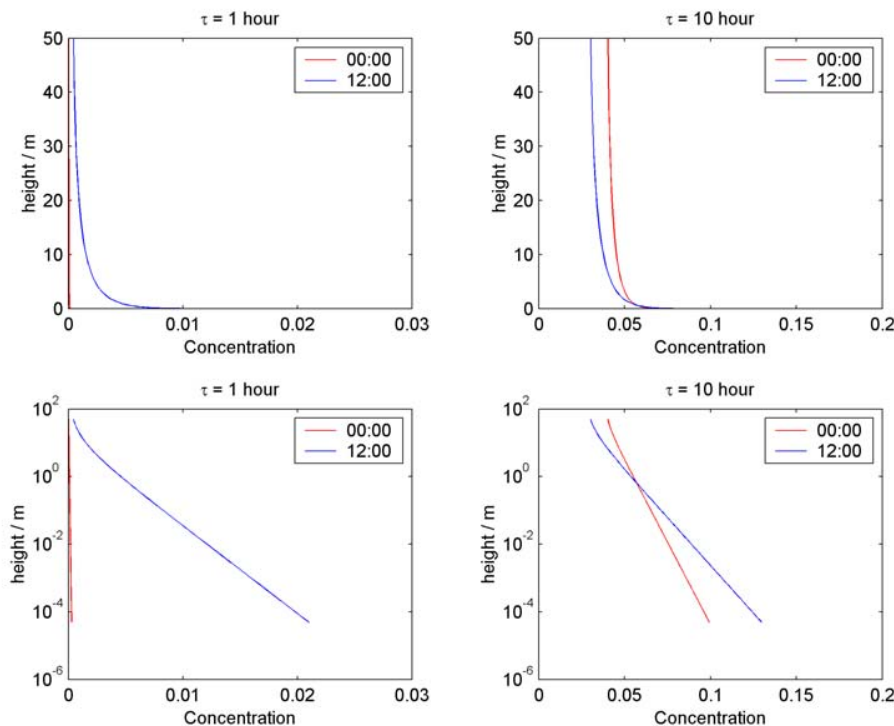
Fig. 4. Profiles of diffusion model concentration at midnight and midday for different values of loss term, τ and with diurnal variation in tracer flux at the surface The profiles are plotted with both linear and log height axes. Note the change in scale for the concentration for the different values of τ.

EGU

Boundary layer physics over snow and ice

P. S. Anderson and W. D. Neff
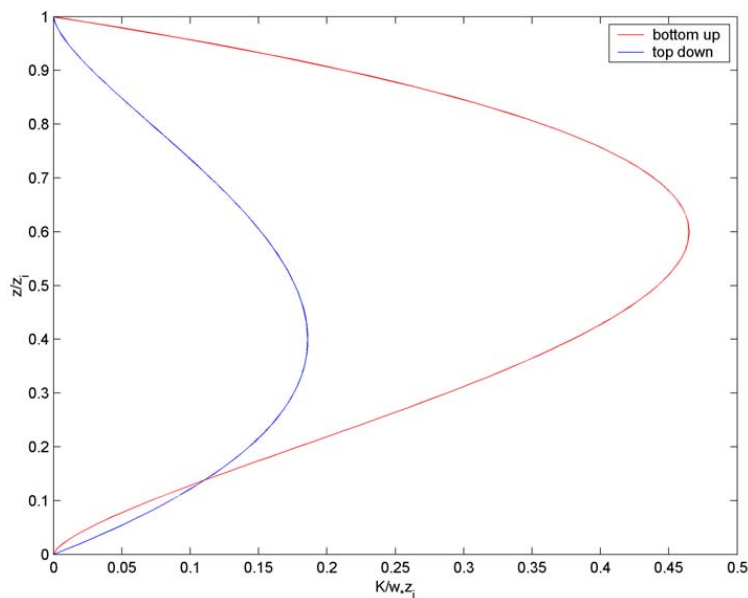
Fig. 5. Idealised and normalised diffusion curves for convection showing difference between upward and downward diffusion.
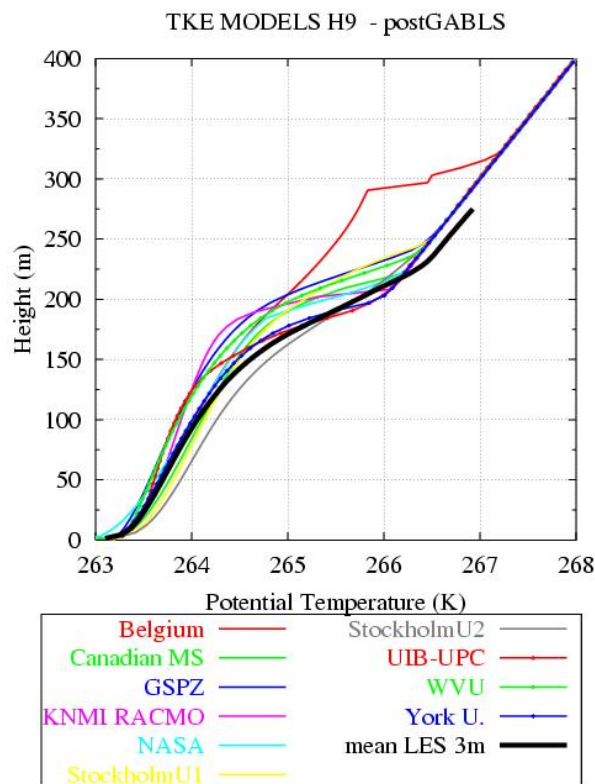
Fig. 6. Comparison of temperature profiles from state-of-the-art 1-D SBL models. Initiated with weak stable gradient, constrained by an explicit gradual surface cooling, fixed geostrophic wind speed and upper level temperature. For this simplest of cases, where only the internal shape of the profile may differ, the various models exhibit a wide range of cooling rates and resultant profile gradients.
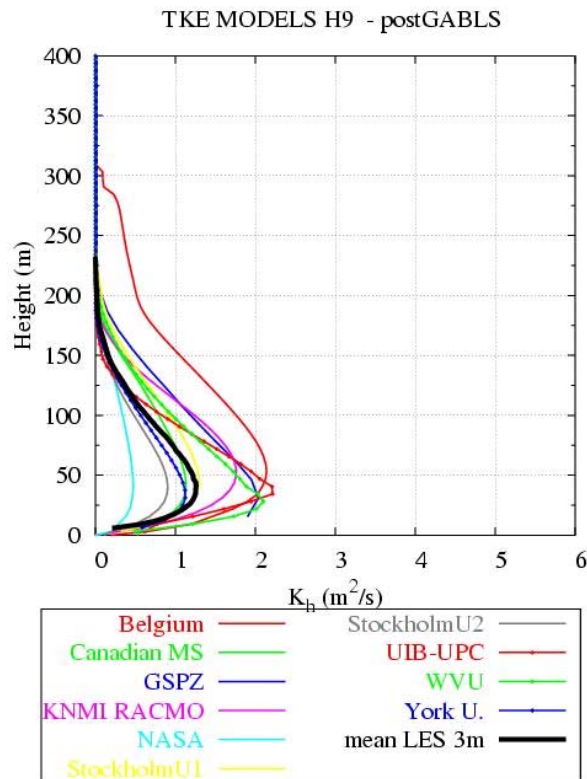
Fig. 7. As for Fig. 6 showing diffusivity profiles. A significant variation in profile shape and maximum diffusivity is apparent, which is of concern given that the model runs were for a fairly moderate stratification, and with fixed upper and lower wind speed and temperature. In real situations, the lower constraints are the controlled by the surface energy balance, and surface temperatures may decrease rapidly.
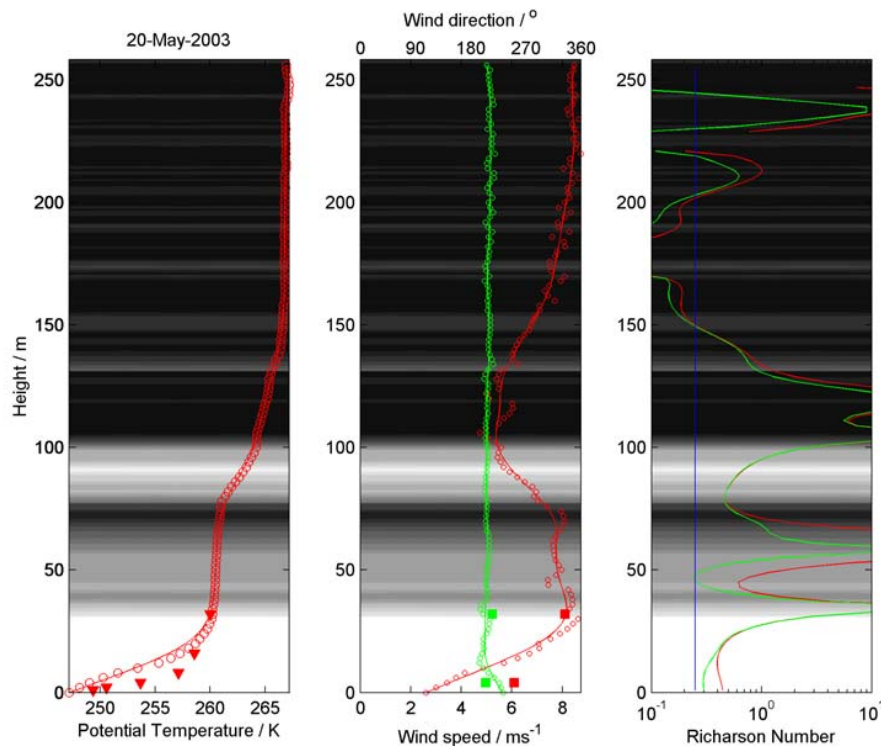
Fig. 8. Profiles of temperature, wind speed and Richardson number for a stable ABL over flat terrain, collected by tethersonde and profile mast at Halley on 19 May 2003. Circles are sonde data, solid lines are the same data smoothed by a 13 point Hamming filter. Triangles are mast mounted aspirated thermometers, squares sonic anemometers. The plots show two levels of mixing depth as might be interpreted from these data. Firstly, the "top of inversion" and low level jet maximum are somewhere between 20 m and 30 m, whilst there is still mixing apparent up to 80 m interpreted from the residual temperature gradient and low Ri. The background shading is C_T^2 (sodar echo strength) implying mixing occurs up to 75 m.

EGU

19-May-2003
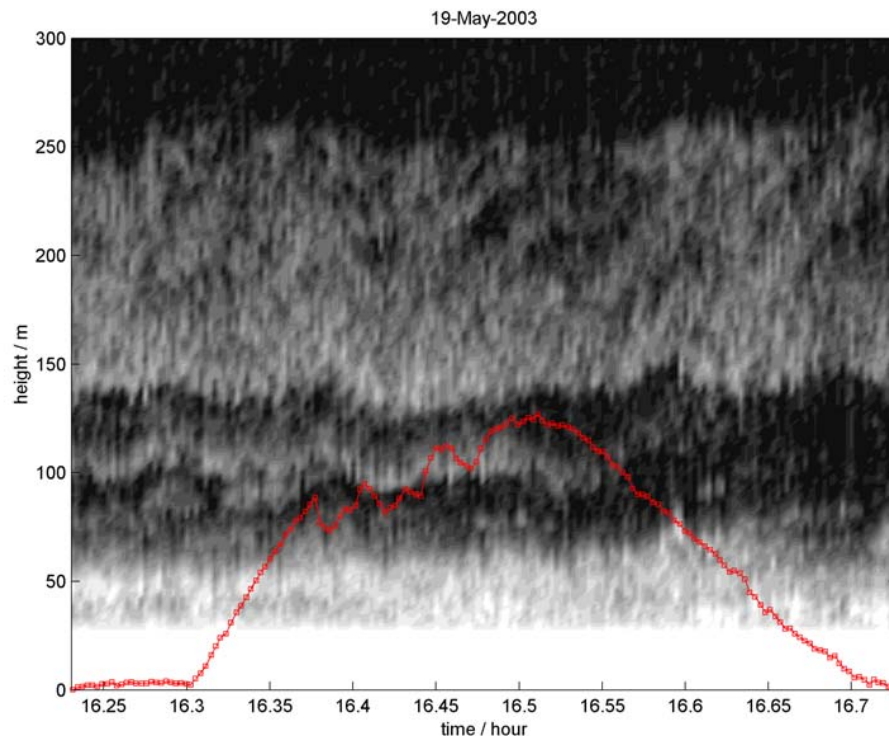
Fig. 9. Sodar echogram for the tethersonde flight in Fig. 8; lighter shading implies stronger echo return from turbulence acting on the temperature gradient. Note that the descent data are presented. The echogramme gives a qualitative indication of mixing depth, h_z, but there is still debate as to exact matching of derived h_z from sodar, temperature or extrapolated turbulence data. The flight position of the sonde is indicated in red.
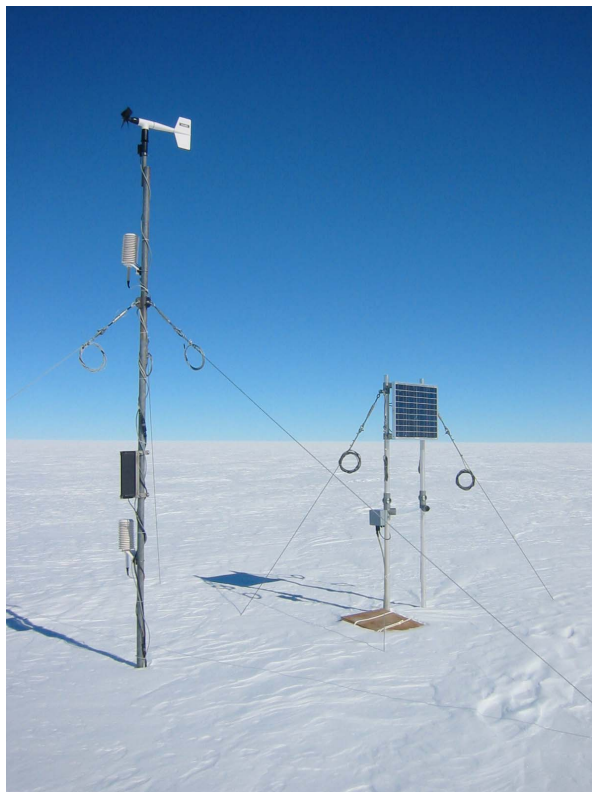
Fig. 10. Typical winter-over polar AWS deployed in Coats Land. Note the propeller-vane anemometer which is less susceptible to icing errors, and the twin temperature sensors (inside radiation shields) to record temperature gradient. The mast is kept free of logging boxes and solar panels to reduce wind flow distortion.

Fig. 11. Four-component radiation sensor on AWS9, at Kohnen Station, Antarctica (CNR1, from Kipp and Zonen). Icing can be a problem on these sensors, but careful cross-analysis of the data can indicate when icing is present. Photo courtesy of M. R. van den Broeke.

Fig. 12. View up a typical boundary layer profile mast, showing (on RHS) mean wind and temperature sensors at 1 ,2 4, 8 16 and 32 m levels. On the left are turbulence sensors, with three sonic anemometers at 4, 16 and 32 m, and an infra-red hygrometer (IRH) at 4 m. The IRH allows moisture flux to be estimated using the co-variance of humidity with the pseudo-co-located turbulence data. Image from Halley, 2003.

Title Page

Abstract | Introduction

Conclusions | References
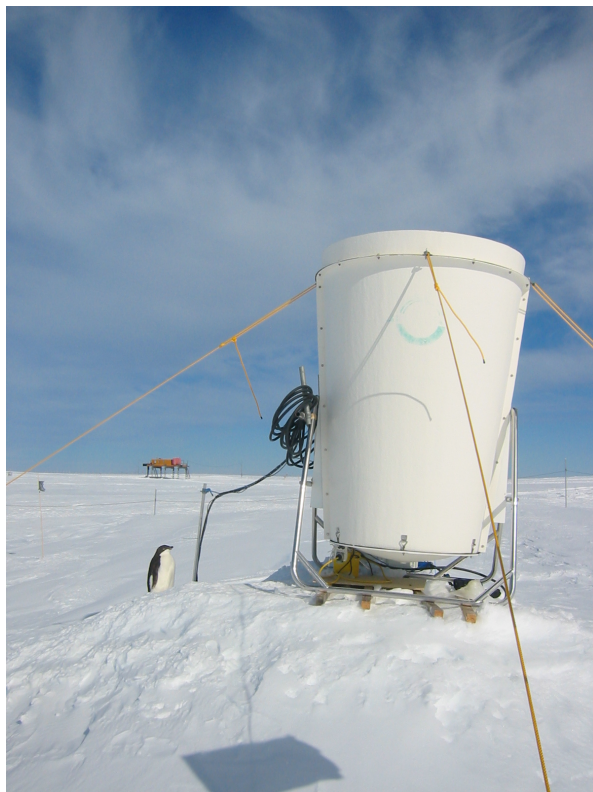
Tables | Figures

◀ | ▶

◀ | ▶

Back | Close

Full Screen / Esc

Printer-friendly Version

Interactive Discussion

Fig. 13. Simple acoustic sounder (sodar) at Halley. The bulk of the antenna is a hollow cone that acts as acoustic shielding to reduce side echoes and background noise: the base is a focusing dish to produce a vertical acoustic beam for transmission and reception. Off-station acoustic sounders are now available, which use an array of small transceivers to produce the same effect. Note that the antenna is off-vertical due to insolation melting the snow berm.

Title Page

Abstract | Introduction

Conclusions | References

Tables | Figures

◀ | ▶▮

◀ | ▶

Back | Close

Full Screen / Esc

Printer-friendly Version

Interactive Discussion

EGU

Fig. 14. The Mavionics T200 UAV and Braunschweig University turbulence instrument package being deployed at Halley during 2007 winter. Civilian/research UAVs are developing rapidly, although they are still a high risk instrument platform requiring a skilled operator. Despite GPS waypoint-following robotics able to fly autonomously out of radio/visual contact, at present these units require piloted (radio controlled) take-off and landing. These issues will resolve in time to provide the boundary layer community with an unprecedented view of the spatial structure of the lower atmosphere. Please note that this image is a montage.

EGU